Article

Service Life Design of Concrete Structures Made of High-Volume Limestone Powder Concrete—Case of the Carbonation-Induced Corrosion

Vedran Carević [1],* , Snežana Marinković [1] , Jasna Plavšić [1] and Andrija Radović [2]

[1] Faculty of Civil Engineering, University of Belgrade, Bulevar Kralja Aleksandra 73, 11000 Belgrade, Serbia; sneska@imk.grf.bg.ac.rs (S.M.); jplavsic@grf.bg.ac.rs (J.P.)
[2] Faculty of Technical Sciences, University of Priština in Kosovska Mitrovica, Knjaza Miloša 7, 38220 Kosovska Mitrovica, Serbia; andrija.radovic@pr.ac.rs
* Correspondence: vedran@imk.grf.bg.ac.rs

Abstract: One of the paths to CO_2 emissions reduction in the concrete industry is to use low-clinker cements, providing at the same time the performance of concrete that is adequate for application in concrete structures. This paper explores the impact of the clinker replacement with high amounts of limestone powder (21–70% in the powder phase) on concrete carbonation resistance. To quantify this impact, the empirical relationship between the carbonation resistance and the compressive strength of the high-volume limestone powder concrete (HVLPC) was established. For that purpose, the regression analysis was applied on the experimental results collected from the published research. The service life analysis based on the full probabilistic approach was performed using the *fib* Model Code 2010 prediction model and proposed empirical relationship. The first-order reliability method (FORM) was applied to solve the limit state function of reinforcement depassivation with a reliability index equal to 1.3. The obtained minimum concrete cover depths were 40–110% higher compared to those prescribed in the current European standard EN 1992-1-1:2004 for indicative strength classes. Based on the full probabilistic analysis, recommended cover depths are given for all carbonation exposure classes, commonly applied concrete strength classes, and service lives of 50 and 100 years.

Keywords: carbonation resistance; high-volume limestone powder concrete; service life design; concrete cover depths

1. Introduction

A key challenge of this century is the need to mitigate and adapt to climate change, and avoid negative impacts on the environment, the economy, and social well-being. Across the globe, the negative impacts of climate change are already recorded and set to continue: higher risks from natural hazards, global sea rise, significant species loss, ocean acidification, etc. [1,2]. To avoid the worst, it is imperative to "hold the increase in the global average temperature to well below 2 °C above pre-industrial levels and to pursue efforts to limit the temperature increase to 1.5 °C above pre-industrial levels" [3]—the main objectives of the flagship Paris Climate Agreement (COP 21). Achieving results with the urgency needed to meet COP 21 commitments requires targeting high-emitting industries and activities. The construction industry largely contributes to Europe's environmental footprint: 50% of natural raw materials use, 40% of total energy consumption [4] (as the single largest consumer), and 36% of all greenhouse gas (GHG) emissions [5], while construction and demolition waste (CDW) makes 46% of the total waste generated [6].

Concrete and other cement-based materials are responsible for a large share of the construction industry's environmental impacts. Concrete is the most widely used construction material in the world, with 33 billion tons produced annually [7]; it is composed of cement, aggregates, water, mineral, and chemical admixtures. Due to the cement (clinker)

production process and the chemical reactions involved, it is responsible for 8–9% of annual anthropogenic CO_2 emissions [8]. Therefore, decarburization of the concrete/cement sector plays an important role in achieving a carbon neutral future.

Decreasing the clinker content by replacing it with so-called supplementary cementitious materials (SCMs) with low embodied CO_2 presents one of the viable solutions to this problem. Today we already use commercial cements with part of the clinker replaced with SCMs: CEM II/A with up to 20% fly ash (FA), ground granulated blast furnace slag (GGBS) and limestone (LS), CEM II/B with up to 35% FA, and GGBS, LS, and CEM III with up to 95% GGBS. Bearing in mind the limited global availability of commonly used SCMs (FA and GGBS) [9], alternative SCMs, abundant in nature, should be looked for. Limestone, if finely ground, can serve this purpose [10]. However, compared to FA and GGBS, it is less effective and has a higher impact on the mechanical and durability-related concrete properties due to its very low reactivity [11–15]. Therefore, higher clinker replacements with limestone powder (>15–20%) present a problem for the structural concrete at all performance aspects.

One of the important durability-related properties of the concrete is its carbonation resistance. This depends mainly on the porosity and pore size distribution on the one hand, and the amount of carbonatable constituents, i.e., alkaline reserve, on the other. On both levels, the limestone powder concrete is inferior to Portland cement concrete due to the dilution effect of the limestone. Several experimental campaigns reported so far in the literature [11,16–19] as well as review papers [20–23] showed that the replacement of the clinker with up to 15% limestone powder practically does not affect the carbonation resistance, while higher replacement ratios reduce it significantly, the reduction being larger with a larger replacement ratio. However, it was shown in the previous research that it was possible to significantly improve the high-volume limestone powder concrete (HVLPC) performance by optimizing the paste composition, lowering the water-to-cement ratio using a larger superplasticizer content, improving the particle packing, and incorporating the nano-calcium carbonate [22,24–31].

Carbonation resistance of the concrete in the concrete cover of reinforced concrete (RC) structures is not an only, but it is a decisive factor for the RC structures' resistance to carbonation-induced corrosion, and therefore their durability. The carbonation-induced corrosion of steel reinforcement is one of the major sources of the RC structures' deterioration—according to Jones et al. [32], two thirds of all structural concrete is exposed to this type of deterioration mechanism.

Modern standards in the construction area tend to rely on the performance-based design for all limit states including durability, as is the case for the *fib* Model Code 2010 [33], for instance. For a performance-based design, it is necessary to have a reliable prediction model for the carbonation-induced reinforcement corrosion. The carbonation process, as mostly a diffusion-controlled process, is usually described with the Fick's first law in the form:

$$x_c = k \cdot \sqrt{t}, \tag{1}$$

where x_c is the carbonation depth, k is the carbonation rate coefficient, and t is time. Unlike that for the concrete with FA and GGBS blended cements [22], very few mathematical prediction models for the limestone powder concrete have been developed so far [11,34,35]. These models are complex and require knowledge on many parameters that influence the carbonation process. For everyday engineering practice, however, simpler models are needed. One such simpler model is given in the previously mentioned *fib* Model Code 2010 [33], originating from the *fib* Model Code for service life design [36]. Although simple, this prediction model requires an experimental determination of the carbonation depth under defined conditions. Therefore, the property that reflects the concrete carbonation resistance has to be experimentally determined. Current European standards EN 12390-10:2018 [37] and EN 12390-12:2020 [38] prescribe the test conditions for determining the carbonation resistance under natural and accelerated conditions, respectively. Tests under natural conditions should last for one year, while for the tests under accelerated conditions, which are shorter (70 days), non-standard laboratory equipment—carbonation chamber—is

required. To avoid this experimental test, finding an empirical relationship with concrete properties that must be tested in any case, such as concrete compressive strength, would significantly improve the feasibility of the model. For the sake of reliability, this relationship would preferably be established for carbonation resistance under natural conditions.

Several authors have already tried to establish such relationships: based on the measured carbonation depths on existing RC structures without information on the exact concrete type [39], or for high volume fly ash and recycled aggregate concrete [40]. Gonçalves et al. [41] reported two different power relationships between carbonation resistance and compressive strength: one for concrete with CEM I and CEM II/A (including CEM II/A-L) and the other for concrete with CEM II/B (but excluding CEM II/B-L(LL)), CEM III, CEM IV, and CEM V. Shah et al. [42] found that a meaningful correlation between the carbonation rate coefficient and compressive strength could not be established due to high scattering. This conclusion was drawn on the basis of their own experimental results and results reported in Rathnarajan et al. [43] and Vu et al. [44], which included concrete mixes with various SCMs (GGBS, FA, calcined clay, limestone, and combinations). On the contrary, Lollini et al. [13] concluded that an exponential relationship between the carbonation rate coefficient and compressive strength existed for concretes with different SCMs, although only based on their own test results. They did not propose specific relationships since consensus on this matter was still lacking according to authors. As for high-volume limestone powder concrete (>20% in the powder phase), one proposal was found in the published research, but for accelerated conditions. Marques et al. [45] proposed a linear relationship between the carbonation rate coefficient and compressive strength for CEM II/B-L concrete (up to 35% limestone powder) based on their own test data with a relatively small range of compressive strengths (between 40 and 50 MPa).

Service life modeling based on physico-chemical prediction models and a full probabilistic approach should give estimates on RC structures' durability that are more realistic compared to the deemed-to-satisfy approach mostly based on the empirical evidence. Several researchers have performed a probabilistic carbonation service life analysis but their results were limited to limestone powder concrete mixes tested in their own investigation [13,45,46]. Neves et al. [47] and Belgacem et al. [48] established an empirical relationship between the accelerated carbonation rate coefficient and air permeability coefficient and performed a probabilistic service life analysis, giving recommendations for the practical design. However, these recommendations were developed on the basis of their own test results on CEM II/A-L concrete mixes and therefore cannot be generalized.

Therefore, a reliable simplified prediction model for carbonation resistance of HVLPC currently does not exist. Models proposed so far in the literature are based either on test results from one laboratory with a small range of involved parameters or include mixes with various SCMs in lower contents. Consequently, it is not possible to design the HVLPC reinforced structure for a prescribed service life, i.e., it is not possible to calculate the required concrete cover depths. Current standards are valid for some of the cements available in the market and these present a serious obstacle to the application of HVLPC in RC structures. In this paper, a simplified prediction model based on test results from 14 different laboratories available in the literature was proposed. Using this empirical model and full probabilistic service life analysis, the HVLPC concrete cover depths for exposure classes XC1–XC4 were also proposed.

2. Objectives

The objectives of this work were:

- To establish the empirical relationship between the carbonation resistance and the compressive strength of the HVLPC (21–70% limestone powder content in the concrete powder phase). The relationship was obtained using the regression analysis applied to the experimental results collected from the published research.

- To propose the concrete cover depths for the HVLPC, depending on the limestone powder content and carbonation exposure class. The service life analysis based on the full probabilistic approach was performed using the *fib* Model Code 2010 [33] prediction model and proposed empirical relationship.

3. Methodology

For describing the carbonation process development with time *t*, the *fib* Model Code 2010 [33] prediction model was used:

$$x_c = k \cdot W(t) \cdot \sqrt{t}, \tag{2}$$

where:

x_c is the carbonation depth (mm);

k is the carbonation rate coefficient (mm/year$^{0.5}$) defined as:

$$k = \sqrt{2 \cdot k_e \cdot k_c \cdot R_{NAC}^{-1} \cdot C_s}, \tag{3}$$

k_e is the environmental function (-);

k_c is the execution transfer parameter (-);

C_s is the CO_2 concentration in the air (kg/m^3);

$W(t)$ is the weather function (-);

R^{-1}_{NAC} is the inverse effective carbonation resistance of concrete under natural conditions ((mm^2/years)/(kg/m^3)).

The inverse effective carbonation resistance R^{-1}_{NAC} reflects the carbonation resistance of concrete depending mostly on the water-to-cement ratio and binder type, while other parameters in Equations (2) and (3) take into account the influence of the environmental and execution conditions. It is recommended in [33,36] that R^{-1}_{NAC} is calculated using R^{-1}_{ACC}, which is experimentally determined under defined accelerated conditions (ACC):

$$R_{NAC,0}^{-1} = k_t \cdot R_{ACC}^{-1} + \varepsilon_t, \tag{4}$$

where:

k_t is the regression parameter for the test effect of the ACC test (-);

ε_t is the error term for inaccuracies that can occur when using the ACC test method ((mm^2/years)/(kg/m^3)).

It was assumed that model (Equations (2) and (3)) is valid for HVLPC as well, except for the inverse effective carbonation resistance that is a material property. In order to establish the empirical relationship between R^{-1}_{NAC} and compressive strength of the limestone powder concrete, experimental results were collected from the previous research in the 1995–2023 period. Collected test results were then filtered to satisfy the following conditions: limestone powder was the only SCM in the concrete mix with more than 20% participation in the powder phase, whether it was contained in the commercial CEM II/B-L(LL) cement or added to CEM I concrete mix in a certain amount; minimal mean compressive strength of concrete f_{cm} on the cylinder was equal to 20 MPa; measured carbonation depth was not less than 1 mm; minimum natural exposure duration was 140 days; all necessary curing and environmental conditions were reported. Since the curing conditions have a large impact on the carbonation front propagation, a minimal curing period of 7 days was adopted. Applying these filters led to 75 experimental results of carbonation depth measured under natural indoor and sheltered outdoor conditions [12,13,16,18,25,26,49–56], on which the regression analysis was performed. Those data originate from 14 different laboratories; however, from some experimental campaigns, only 2 or 3 measured data satisfied the mentioned conditions and were included. The data range is shown in Table 1.

Table 1. Range of concrete and environmental data in analyzed experimental results.

Properties of concrete mix	
Limestone powder content (% of total powder phase)	21–70
Cement type	CEM I or CEM II/B-L(LL)
Curing time (days)	7–28
Mean compressive strength, 28 days, cylinder (MPa)	20–62
Environmental conditions	
RH (%)	60–75
CO_2 concentration (%)	0.035–0.045
Exposure conditions	indoor and outdoor sheltered
Exposure time (days)	>140

After establishing a relationship between $R^{-1}{}_{NAC}$ and f_{cm}, the service life was predicted using Equation (2). By comparing the probability of the carbonation depth reaching the nominal concrete cover depth (c_{nom}), the limit state function of reinforcement depassivation can be written in the following form:

$$g(c_{nom}, x_c(t)) = c_{nom} - x_c(t) = c - \sqrt{2 \cdot k_e \cdot k_c \cdot R_{NAC}^{-1} \cdot C_s \cdot t} \cdot W(t), \tag{5}$$

The first order reliability method (FORM) was applied to calculate the limit function for the defined probability of failure. However, for the calculation of the limit state function, it is necessary to define the distribution parameters for each variable in Equation (5).

Given that concrete cover is a stochastic variable, it can be described with a lognormal distribution, bearing in mind that it cannot have negative values. The nominal concrete cover (c_{nom}), defined in EN 1992-1-1:2004 [57], represents the mean value of the concrete cover depths (see Table 2). It consists of the minimum cover necessary to protect the reinforcement from corrosion ($c_{min,dur}$) increased by an absolute value of the accepted negative deviation (Δc_{dev}), which depends on the quality of execution works. For cast-in-situ structures, the prescribed Δc_{dev} is 10 mm. It is reasonable to assume that the concrete cover standard deviation (σ_c) is controlled by the execution requirements, which are often interpreted as 5% quantile of concrete cover values [58]:

$$\sigma_c = \frac{\Delta c_{dev}}{1.645} = 6 \; mm, \tag{6}$$

Table 2. The nominal concrete cover depths for service lives of 50 and 100 years according to [57].

	Service Life (t_{SL})	Exposure Class			
		XC1	XC2	XC3	XC4
c_{nom} (mm)	50 years	25	35	35	40
	100 years	35	45	45	50

The coefficient k_e represents the environmental conditions:

$$k_e = \left(\frac{1 - (RH_{real}/100)^{f_c}}{1 - \left(RH_{ref}/100\right)^{f_c}} \right)^{g_c}, \tag{7}$$

where RH_{real} is the environmental relative humidity (%), RH_{ref} is the referent relative humidity (65%), f_c is an exponent (5.0), and g_c is another exponent (2.5).

Distribution parameters for the environmental relative humidity were adopted according to previous studies [59,60], for each exposure class defined in EN 1992-1-1:2004 [57]. The execution transfer parameter (k_c) represents the curing conditions and is defined as:

$$k_{cur} = \left(\frac{t_c}{7}\right)^{b_c},$$

(8)

where t_c is the curing period (days), and b_c is the regression exponent (-).

The curing period (t_c) of 7 days was adopted assuming that this is the standard on-site curing period. It is also the time defined in the *fib* Model Code for service life design [36] for the accelerated carbonation test. The distribution parameters of the exponent b_c were adopted according to the recommendation from the same document [36]. In addition, the distribution parameters for the CO_2 concentration (C_s) were adopted according to values defined in [36], taking into account the constant increase in concentration in the past century. For the weather function $W(t)$, the maximum value (1.0) was taken, given that only indoor and sheltered-from-rain samples were analyzed in this study. Finally, the distribution of predicted R^{-1}_{NAC} was calculated according to the procedure explained in Section 4.2. The summary of all input parameters is shown in Section 4.3.

To solve the limit state function defined in Equation (5), it is necessary to define the required minimum reliability index (β). Here, the value of 1.3 ($P_f \leq 0.10$) was adopted as per the *fib* Model code for the service life design [36] requirement for the depassivation limit state. A service life of 50 and 100 years was used in the calculations. By solving the limit state function defined in Equation (5), it is possible to obtain the required concrete cover depth for the defined parameters, or to determine the service life for the defined concrete cover.

4. Results and Discussion

4.1. Relationship between R^{-1}_{NAC} and Compressive Strength of the Limestone Powder Concrete

In the analyzed literature, experimental results were reported either as the measured carbonation depth x_c or carbonation rate coefficient k; in the latter case, carbonation depth was calculated using Equation (1).

The inverse effective carbonation resistance of concrete, determined under natural conditions (natural carbonation test—NAC) was calculated from Equations (2) and (3):

$$R^{-1}_{NAC} = \frac{x_c(t)^2}{2 \cdot k_e \cdot k_c \cdot C_s \cdot t \cdot W(t)},$$

(9)

using the reported curing and exposure conditions and measured carbonation depths. Values of R^{-1}_{NAC} calculated in that way and the reported compressive strengths were considered as mean values.

Concrete mixes were divided into two groups according to limestone percentage: (1) between 21% and 35%, and (2) between 36% and 70% limestone powder in the concrete mix. The limestone percentage was calculated as the ratio between the limestone amount and the powder phase amount (Portland cement + limestone powder). Such division was adopted in order to differentiate between the limestone content available in commercial cement CEM II/B-L(LL) and higher limestone content.

The relationship between R^{-1}_{NAC} and f_{cm} was best described with the power regression model. However, reducing the power regression to the linear regression model of the log-transformed variables offers a simpler mathematical tool for further application. The linear model of the log-transformed variables is:

$$\ln R^{-1}_{NAC} = b_1 \cdot \ln f_{cm} + b_0,$$

(10)

where b_0 and b_1 are the linear regression coefficients representing intercept and slope, respectively.

The results are shown in Figures 1 and 2 for concrete mixes with between 21% and 35%, and between 36% and 70% limestone powder, respectively. Since the models did not differ substantially, an additional model for the concrete mix with limestone content between 21% and 70% was also estimated and shown in Figure 3. The coefficient of determination R^2 for the linear regression models of log-transformed variables ranges between 0.76 and 0.80 depending on the mix (Table 3). The coefficient estimates, their standard errors, and significance are also given in Table 3. The null hypotheses that $b_0 = 0$ and $b_1 = 0$ can both be rejected for all mixes at virtually any significance level. Each regression model was also shown to have independent, homoscedastic, and normally distributed residuals. The normality of the residuals was tested by applying the Kolmogorov–Smirnov goodness-of-fit test at the 5% significance level. Figures 1–3 also show the 90% confidence intervals for predicted values of R^{-1}_{NAC}.
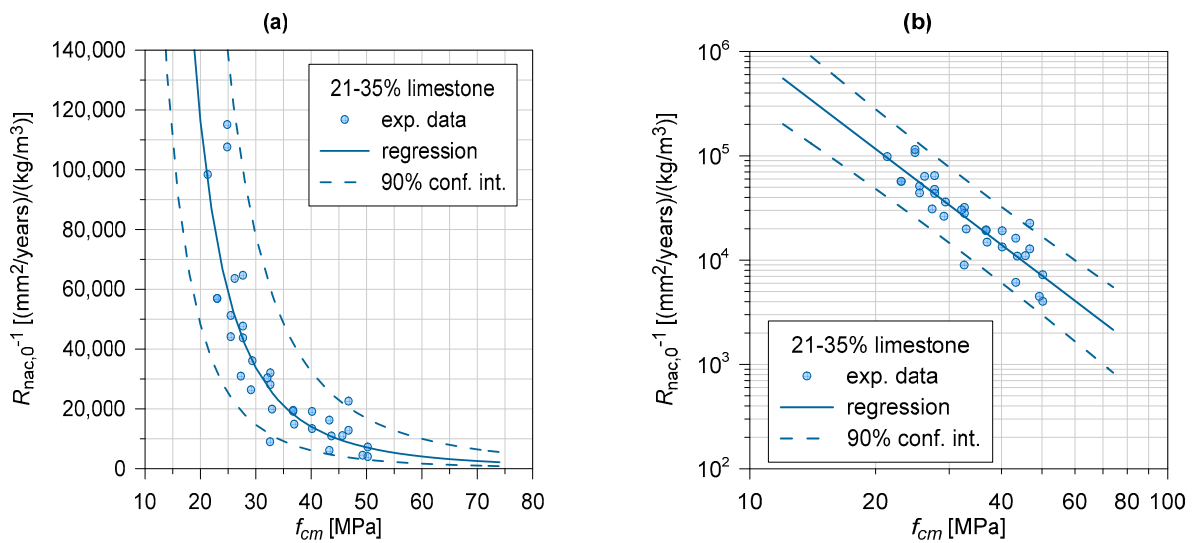
Figure 1. Relationship between the natural inverse carbonation resistance and mean compressive strength of concrete for mixes with 21–35% limestone powder: (**a**) power regression and (**b**) linear regression of log-transformed variables.

Figure 2. Relationships between the natural inverse carbonation resistance and mean compressive strength of concrete for mixes with 36% to 70% limestone powder: (**a**) power regression and (**b**) linear regression of log-transformed variables.
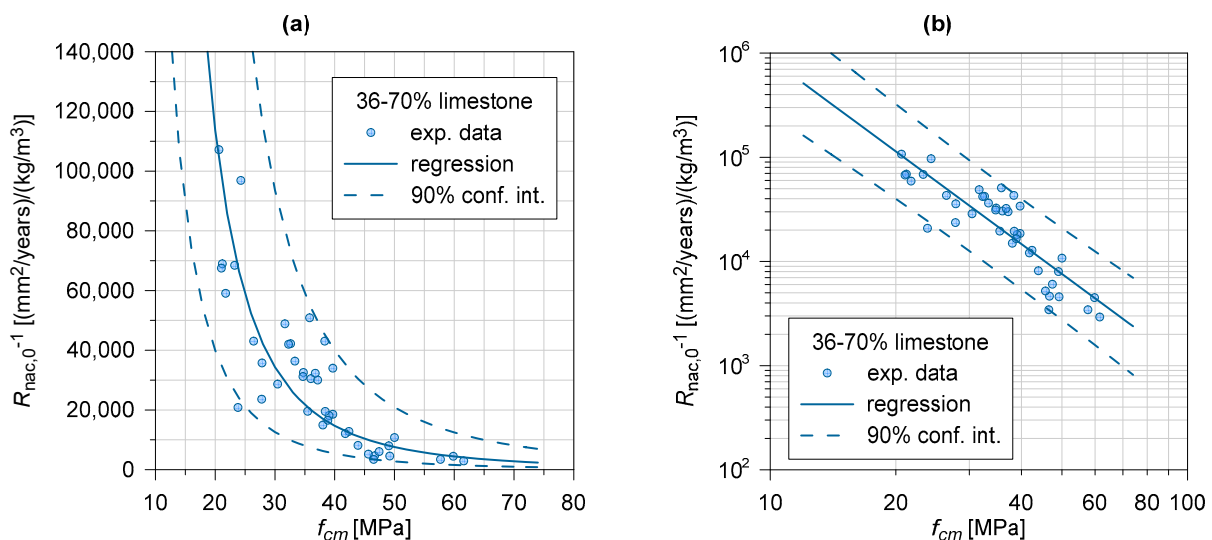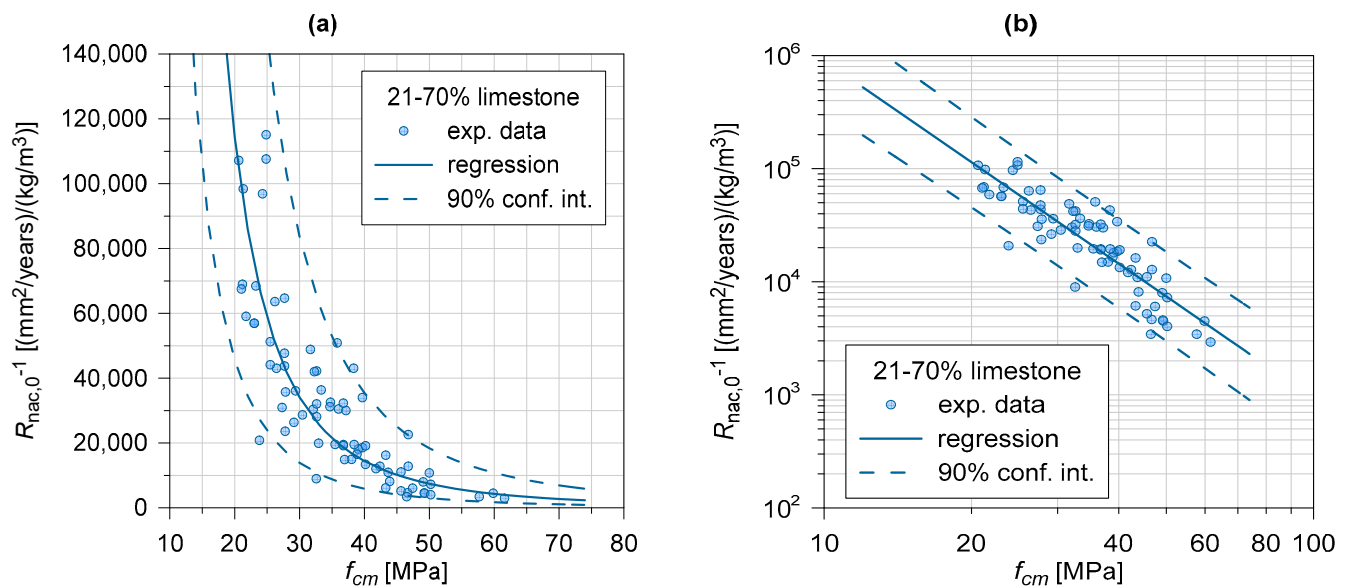
Figure 3. Relationships between the natural inverse carbonation resistance and mean compressive strength of concrete for mixes with 21% to 70% limestone powder: (**a**) power regression and (**b**) linear regression of log-transformed variables.

Table 3. Linear regression of R^{-1}_{NAC} on $\ln f_{cm}$: model adequacy as measured by coefficient of determination, estimated coefficients, and their properties.

Concrete Mix (Limestone Content)	21–35%	36–70%	21–70%
Number of data	33	42	75
Coefficient of determination, R^2	0.80	0.76	0.78
Slope coefficient, b_1			
estimate	−3.050	−2.9534	−2.9839
standard error	0.2739	0.2640	0.1877
significance (*p*-value)	<<0.001	<<0.001	<<0.001
Intercept, b_0			
estimate	20.801	20.489	20.585
standard error	0.9627	0.9473	0.6674
significance (*p*-value)	<<0.001	<<0.001	<<0.001

From this analysis, the relationship between the natural inverse carbonation resistance and mean compressive strength of the limestone powder concrete can be proposed in the following way (with strong correlation, R^2 between 0.76 and 0.8):

$$\ln R^{-1}_{NAC} = -3.05 \cdot \ln f_{cm} + 20.80, \tag{11}$$

for 21% to 35% limestone powder concrete, including commercial CEM II/B-L(LL) cement, and:

$$\ln R^{-1}_{NAC} = -2.95 \cdot \ln f_{cm} + 20.49, \tag{12}$$

for 36% to 70% limestone powder concrete.

As already mentioned, since the relationships for mixes with 21–35% and 36–70% limestone powder are very similar, a single relationship can be proposed for the whole range of 21% to 70% limestone powder, Figure 3:

$$\ln R^{-1}_{NAC} = -2.98 \cdot \ln f_{cm} + 20.59, \tag{13}$$

for 21% to 70% limestone powder concrete, including commercial CEM II/B-L(LL) cement, with statistical parameters of the linear regression model given in Table 3.

The carbonation resistance depends mainly on the porosity and amount of carbonatable constituents. As already mentioned, HVLPC has lower carbonation resistance compared to pure-clinker concrete due to the low reactivity of limestone powder on the one hand, and low clinker content on the other. The first problem (porosity) can be resolved with a properly designed mix even with high limestone powder content, i.e., very good compressive strength can be achieved. For that, it is necessary to optimize the HVLPC mix design, which can be completed in several ways. The most effective way is to use a low content of water and in that way keep the water-to-clinker ratio in limits that do not significantly decrease the strength [24–26]. Since the water content required for adequate workability is usually above the content needed for full clinker hydration, relatively high amounts of plasticizer are needed to keep this excess water at a minimum. Secondly, use of the finely ground limestone improves particle packing density and density of the ITZ (filler effect). Mixing limestone powders of different fineness can also contribute to compressive strength for the same reasons [24]. Finally, adding the limestone powder in contents larger than that for the simple replacement of clinker increases the total powder paste volume, and improves filling of the voids and workability at the same time [27]. Most of the mixes in the database with limestone powder content higher than 35% were designed in that way and achieved compressive strength higher than 30 MPa, even at clinker contents as low as 150–180 kg/m^3. The second problem, a low amount of carbonatable constituents, depends mainly on the clinker content: the lower the clinker content, the lower the alkaline reserve. Due to low $Ca(OH)_2$ content, the carbonation rate is faster, i.e., carbonation resistance is lower and the mix optimization methods mentioned here cannot help. For that reason, HVLPC has lower carbonation resistance compared to pure-clinker concrete for the same compressive strength. The obtained results are: the similar relationships (11) and (12) for 21–35% and 36–70% limestone powder groups, respectively, mean that the impact of porosity, which dictates CO_2 diffusivity, prevails over the impact of the available alkaline reserve.

Keeping in mind the broad range of limestone powder contents (21–70%), the correlation (13) described with the R^2 equal to 0.78 can be considered strong enough for the simplified prediction model. It is important to note that the proposed equations are valid for concrete mixes that are wet-cured for at least 7 days. If shorter curing periods were included (1 and 3 days), a single relationship with a strong correlation between inverse natural carbonation resistance and compressive strength could not be obtained due to the significant impact of short periods on the carbonation resistance. This was however considered acceptable for the simplified prediction model. Moreover, curing periods shorter than 7 days are not likely in practice—they are rather an exception to the rule in special cases.

4.2. Distribution of Predicted $R^{-1}{}_{NAC}$ for Selected Values of Mean Compressive Strength

Logarithmic transformation of the natural inverse carbonation resistance and the mean compressive strength as the regression variables was used to formulate the linear regression model given in Equation (10). This allowed us to establish the regression line as the expected response of $\ln R^{-1}{}_{NAC}$ for a given $\ln f_{cm}$, as well as to compute the prediction (confidence) interval for the values of $\ln R^{-1}{}_{NAC}$ for a given $\ln f_{cm}$. While this procedure is straightforward for linear regression, interpretation of the results with log-transformed variables needs careful consideration. For the sake of clarity, we use the following notation: $y = \ln R^{-1}{}_{NAC}$ and $x = \ln f_{cm}$.

In simple linear regression, the prediction interval is symmetric around the regression line (see Figure 1b, for example). This follows from the regression theory, which postulates that the residuals are normally (symmetrically) distributed with zero mean and variance σ^2. Consequently, predicted response variable y is also normally distributed with conditional mean being the regression line and with the same variance σ^2. Furthermore, the least-squares estimators of regression coefficients $\hat{b}_0$ and $\hat{b}_1$ are random variables by their nature. The variability of $\hat{b}_0$ and $\hat{b}_1$ means that the estimated regression line (10) may deviate from a true one in terms of both slope and intercept. For a fixed value of the explanatory

variable $x = x_0$, the estimated conditional mean response $\mu_{Y|X=x_0} = \hat{b}_1 \cdot x_0 + \hat{b}_0$ is normally distributed as:

$$\mu_{Y|X=x_0} \sim N\left(b_1 x_0 + b_0, \sigma^2\left[\frac{1}{n} + \frac{(x_0 - \overline{x})^2}{S_{xx}}\right]\right), \tag{14}$$

where $\overline{x}$ is the mean value of the explanatory variable, S_{xx} is the sum of squares of x, b_1 and b_0 are true regression coefficients, and n is the number of observations. The variance of the estimated prediction of the response variable $\hat{y}_0$ for the given x_0 is obtained by combining the variances of the estimated regression model and the variance of the residuals ε:

$$\text{var}[\hat{y}_0] = \text{var}\left[\hat{b}_1 x_0 + \hat{b}_0\right] + \text{var}[\varepsilon] = \sigma^2\left[1 + \frac{1}{n} + \frac{(x_0 - \overline{x})^2}{S_{xx}}\right], \tag{15}$$

The above variance is used to compute the $100(1 - \alpha)\%$ confidence intervals for the predicted value y_0 of the response variable:

$$y_0 \in \left(\hat{b}_1 x_0 + \hat{b}_0 - t_{n-2,1-\alpha/2}\sqrt{\text{var}[\hat{y}_0]}, \hat{b}_1 x_0 + \hat{b}_0 + t_{n-2,1-\alpha/2}\sqrt{\text{var}[\hat{y}_0]}\right), \tag{16}$$

where $t_{n-2,1-\alpha/2}$ is the Student's t variate with $n - 2$ degrees of freedom and probability $1 - \alpha/2$. The confidence interval of log-transformed R^{-1}_{NAC} that is symmetric due to the normality assumption becomes asymmetric after exponentiation:

$$R^{-1}_{NAC} \in \left(\exp\left\{\hat{b}_1 x_0 + \hat{b}_0 - t_{n-2,1-\alpha/2}\sqrt{\text{var}[\hat{y}_0]}\right\}, \exp\left\{\hat{b}_1 x_0 + \hat{b}_0 + t_{n-2,1-\alpha/2}\sqrt{\text{var}[\hat{y}_0]}\right\}\right), \tag{17}$$

It should be noted, however, that the inverse transformation (exponentiation) of the linear regression equation does not yield the conditional mean response in the space of the original variable. Since the predicted $\ln R^{-1}_{NAC}$ for the given x_0 is normally distributed, the predicted R^{-1}_{NAC} is log-normally distributed. When exponentiated, the mean value of the log-normal distribution is not equal to the mean value of the normal distribution, although it is equal to the median value of normal distribution [61]. Therefore, the power curves shown in Figures 1a, 2a and 3a do not represent the mean predicted response of R^{-1}_{NAC}, but the median predicted response. The lower and upper confidence limits of the asymmetric 90% confidence interval in Figures 1a, 2a and 3a represent the same probabilities (5% and 95%) of the conditional distribution as in Figures 1b, 2b and 3b.

With log-normally distributed values of the predicted R^{-1}_{NAC} for the given f_{cm}, the relationship between the moments of the original and log-transformed normal variables was used to define the mean and variance of estimated R^{-1}_{NAC} prediction for the given f_{cm} as:

$$\mu_{\hat{R}} = \exp\left\{\mu_{\hat{y}_0} + \sigma^2_{\hat{y}_0}/2\right\}, \quad \text{var}\left[\hat{R}\right] = \mu^2_{\hat{R}}\left[\exp\left\{\sigma^2_{\hat{y}_0}\right\} - 1\right], \tag{18}$$

where $\hat{R}$ denotes the estimated R^{-1}_{NAC} prediction and $\hat{y}_0$ denotes the estimated $\ln R^{-1}_{NAC}$ prediction for the given x_0, i.e., for the given f_{cm}. This allows for computing the moments of the estimated R^{-1}_{NAC} prediction for selected values of f_{cm} and using them in the original space of R^{-1}_{NAC} for the service life analysis. Distribution parameters for R^{-1}_{NAC} have been determined for commonly applied concrete classes defined in EN 1992-1-1:2004 [57]. The distribution parameters, concrete classes, as well as the corresponding f_{cm} are shown in Table 4 for the 21–70% limestone powder concrete since service life analysis was performed for this group of concrete mixes.

Table 4. Moments of conditional log-normal distribution of predicted natural inverse carbonation resistance $R^{-1}{}_{NAC}$ for the selected values of the mean compressive strength f_{cm}.

Concrete Mix (Limestone Content)	Concrete Class	f_{cm} [MPa]	Prediction of $R^{-1}{}_{NAC}$ ((mm²/Years)/(kg/m³))		
			Mean	Standard Deviation	CV (−)
21–70%	C20/25	28	46,342	22,034	0.475
	C25/30	33	28,362	13,433	0.474
	C30/37	38	18,620	8826	0.474
	C35/45	43	12,885	6131	0.476
	C40/50	48	9290	4445	0.479

4.3. Service Life Analysis

A summary of the input parameters for the limit state function of carbonation-induced depassivation is shown in Table 5. Obtained results of the FORM analysis are presented as relationships between the reliability index and period of reinforcement depassivation. Comments are also given regarding the requirements of the currently valid standard EN 1992-1-1:2004 [57]. Figure 4 shows this relationship for a 50-year service life (t_{SL}) concrete cover (c_{nom}) for all exposure classes (XC1–XC4).

Table 5. Input parameters for the limit state function of reinforcement depassivation.

Parameter		Distribution	μ	σ	Unit
c_{nom}		Lognormal	Table 2	6	mm
RH_{real}	XC1	Beta	92 (40 *)	6 (100 *)	%
	XC2	Beta	79 (40 *)	9 (100 *)	%
	XC3	Beta	65 (40 *)	10 (100 *)	%
	XC4	Beta	75 (40 *)	16 (100 *)	%
RH_{ref}		Constant	65	−	%
f_c		Constant	5.0	−	−
g_c		Constant	2.5	−	−
t_c		Constant	7	−	days
b_c		Normal	−0.567	0.024	−
C_s		Normal	0.0008	0.0001	kg/m³
t		Constant	1 ÷ 100	−	year
$R^{-1}{}_{NAC}$		Normal	Table 4		(mm²/year)/(kg/m³)

* Lower and upper limit of the beta distribution.

For exposure class XC1, HVLPC mixes showed that the period of carbonation-induced reinforcement depassivation was 16 years for concrete class C20/25, which is defined as an indicative minimum concrete strength class [57]. As the strength class increased, so did the service life. Although exposure class XC1 was the least aggressive environment, concretes up to class C30/37 did not meet the service life of 50 years (the highest depassivation period was 40 years). Concrete class C35/45 was the first to achieve a service life of 50 years with the prescribed concrete cover (t_{SL} = 57 years). With a further increase in strength, the service life increased up to 79 years for the C40/50 concrete class. By solving the limit state function for the depassivation period of 50 years, the obtained concrete cover depth for strength class C20/25 was 42 mm, instead of the prescribed 25 mm [57].
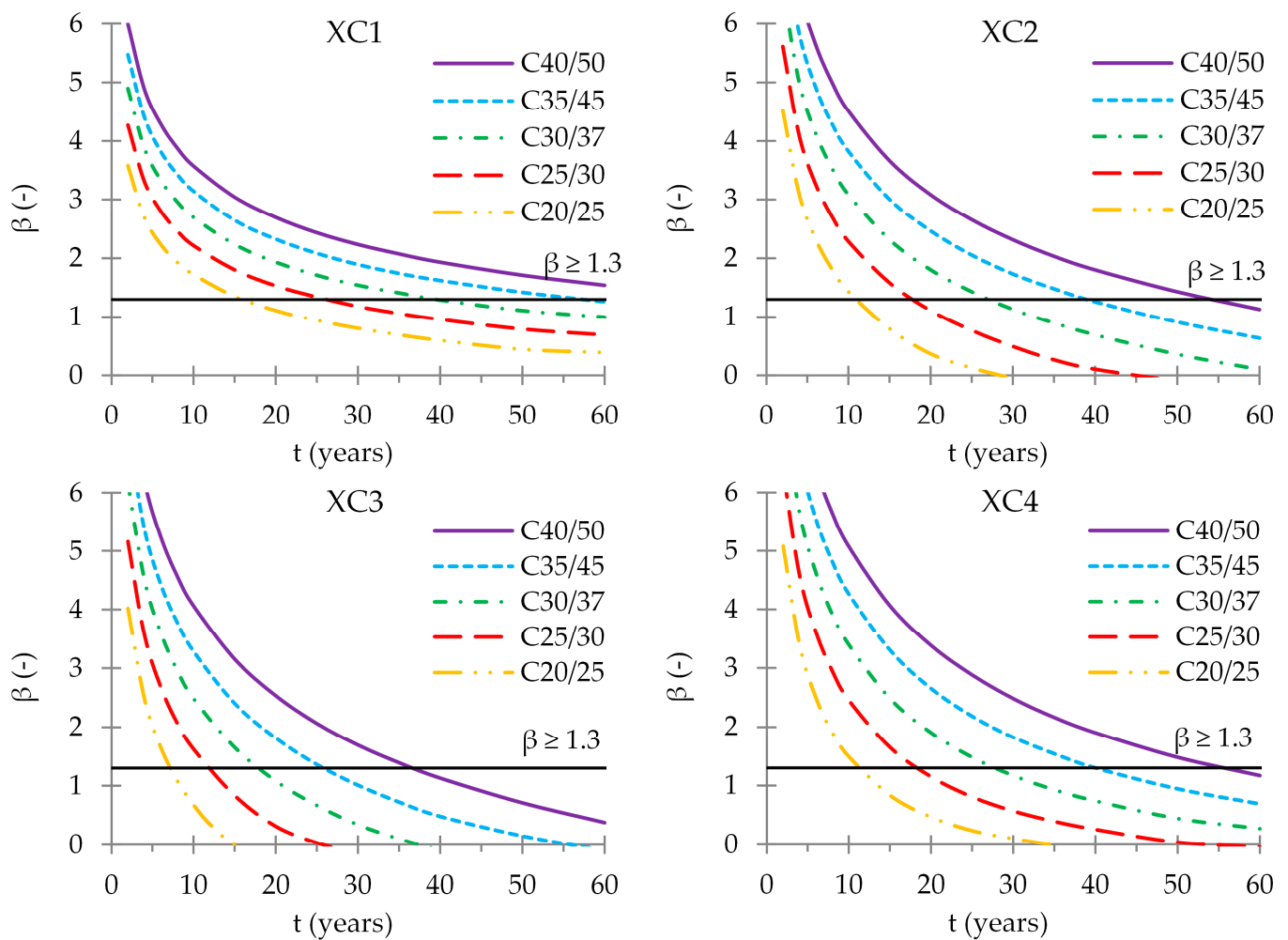
Figure 4. Reliability index (β) values during time of exposure for 50-year service life concrete covers (c_{nom}) and different exposure classes.

A similar situation was observed for exposure class XC2, with the indicative strength class C25/30 and the minimum concrete cover of 35 mm proposed in [57]. For this concrete class, the service life was 18 years. The required service life would be achieved with a concrete cover of 56 mm (21 mm higher than the prescribed value). The only concrete class that satisfied the service life of 50 years was the class C40/50 (54 years).

A higher indicative minimum concrete strength class is prescribed for higher exposure classes. Concrete class C30/37 is prescribed as minimum indicative [57] for classes XC3 and XC4. For exposure class XC4, the values of the service life were similar to those for class XC2, for all concrete classes. The differences in service life duration were up to 1 year. This is not surprising because a 5-mm-higher cover depth is prescribed for the exposure class XC4 as being more prone to carbonation compared to class XC2. The required service life for class C30/37 would be achieved with a concrete cover of 52 mm (12 mm higher than the prescribed value).

The exposure class XC3 had the lowest service life, because moderate humidity represents the most aggressive environment for carbonation development. Although wetting and drying cycles, as defined for exposure class XC4, slow down the carbonation process compared to moderate humidity [59,60], a 5-mm-higher concrete cover depth is also prescribed compared to class XC3 [57]. The higher prescribed concrete cover depth for class XC4 is a consequence of taking into account the possibility of rapid corrosion progress after depassivation has been reached [60], which was not considered as a part of the service life in this study. For exposure class XC3, not a single concrete strength class met the service

life of 50 years with the prescribed concrete cover depth of 35 mm. The required concrete cover depth to satisfy the service life of 50 years, for the prescribed concrete class C30/37, was 56 mm (21 mm more than the prescribed value).

In total, the concrete cover depths for HVLPC mixes were larger by 12 to 21 mm (depending on the exposure class) compared to the prescribed covers in EN 1992-1-1:2004 [57]. The reason for this is their lower carbonation resistance due to the binder dilution caused by replacing the clinker with limestone [23].

Bearing in mind that in EN 1992-1-1:2004 [57] a service life of 100 years is achieved by increasing the concrete cover depth to only 10 mm (Table 2), the depassivation period for this service life duration was also analyzed. Figure 5 shows the relationships between the reliability index and period of reinforcement depassivation for a prescribed 100-year service life of a concrete cover (c_{nom}) for all carbonation exposure classes.
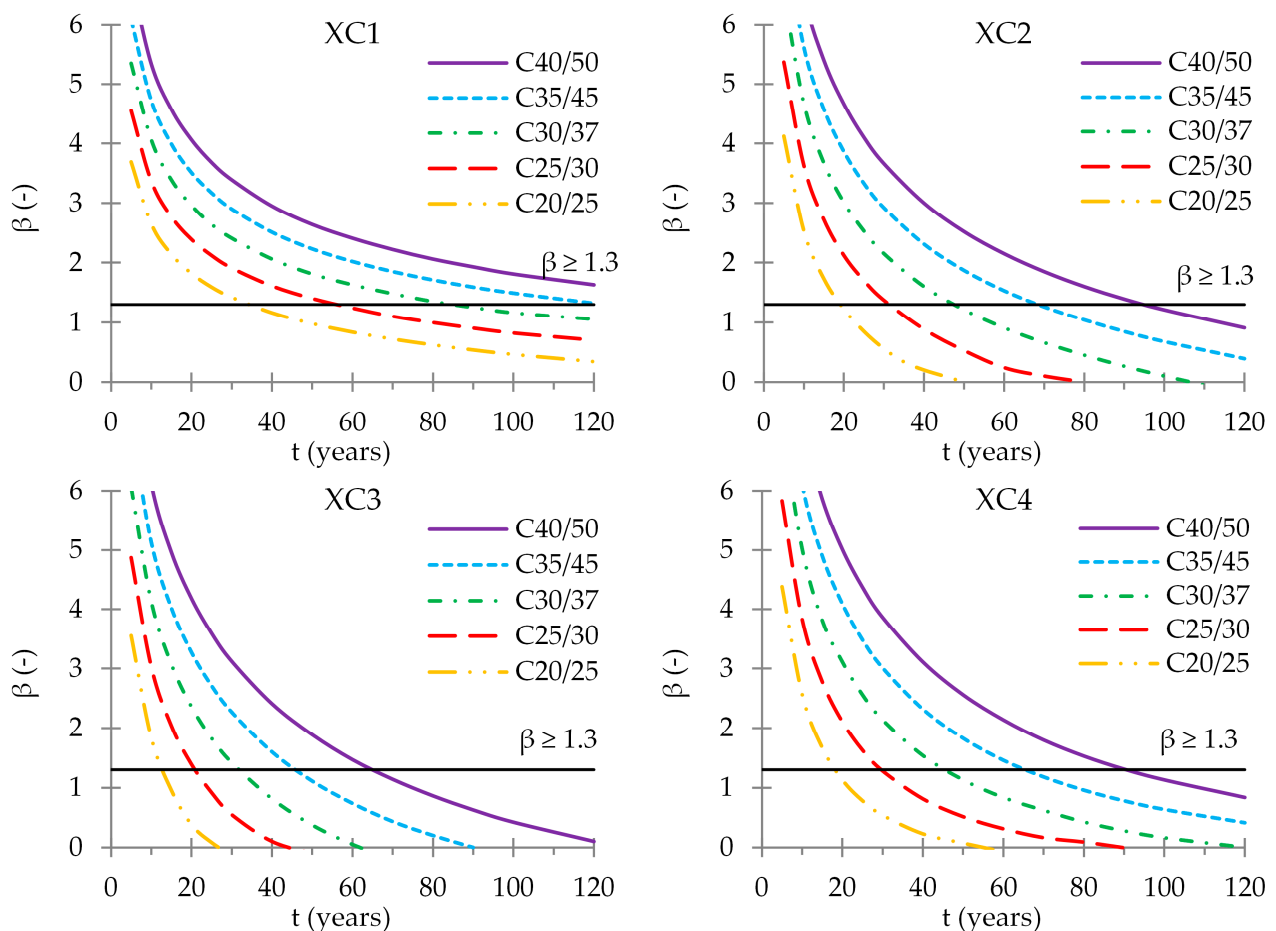

Figure 5. Reliability index (β) during time of exposure for a 100-year service life concrete cover (c_{nom}) and different exposure classes.

For exposure class XC1, the period of depassivation was only 34 years for the indicative minimum concrete strength class C20/25. The required concrete cover depth for this strength class and for a depassivation period of 100 years was 58 mm, 23 mm higher than the prescribed value [57]. With increased concrete strength, the service life also increased. Although exposure class XC1 was the least aggressive environment, as in the case of the service life of 50 years, only the concrete classes C35/45 and C40/50 met the service life of 100 years.

A similar service life was obtained for both XC2 and XC4 exposure classes. Only the C40/50 concrete class had a depassivation period of nearly 100 years. In the case of exposure class XC2, the depassivation period for indicative minimum concrete strength

class C25/30 was 31 years. The required service life for this strength class would be achieved with a concrete cover of 78 mm (33 mm higher than the prescribed value and 22 mm higher than the required 50-year concrete cover). The depassivation period for concrete class C30/37 in the case of exposure class XC4 was 45 years. The required concrete cover depth to satisfy the service life of 100 years was 73 mm (32 mm more than the prescribed value and 21 mm higher than the required 50-year concrete cover).

HVLPC mixes had the smallest depassivation period for exposure class XC3. Not a single concrete class met the service life of 100 years. The longest service life was obtained for the highest strength class C40/50 and it was 65 years. The depassivation period for the indicative minimum strength class C30/37 was only 32 years. The required concrete cover depth to satisfy the service life of 100 years was 77 mm (32 mm more than the prescribed value and 21 mm higher than the required 50-year concrete cover).

The analysis showed that in order to ensure a service life of 100 years, it is necessary to increase the 50-year concrete cover depth by approximately 20 mm in the case of HVLPC. The concrete cover depths were 23 mm larger for classes XC1 and XC4, i.e., 32 mm for classes XC2 and XC3, compared to the prescribed covers in EN 1992-1-1:2004 [57]. Calculated values of the minimum concrete cover depths ($c_{min,dur}$) from the durability point of view for commonly applied concrete classes are shown in Table 6. Given that the calculation was made with the nominal cover depth (c_{nom}), as explained in the Methodology, the minimum cover depth was calculated by reducing the nominal value by the value of the accepted negative deviation (Δc_{dev}).

Table 6. Recommended values of minimum concrete cover depths ($c_{min,dur}$) for 21% to 70% limestone powder concrete and different exposure classes.

	Concrete	Exposure Class			
Service Life	Class	XC1	XC2	XC3	XC4
50 years	C20/25	32 (15 *)	61	75	71
	C25/30	23	46 (25 *)	57	54
	C30/37	18	36	46 (25 *)	42 (30 *)
	C35/45	14	29	37	34
	C40/50	11	24	30	28
100 years	C20/25	48 (25 *)	89	110	103
	C25/30	36	68 (35 *)	84	79
	C30/37	28	54	67 (35 *)	63 (40 *)
	C35/45	22	44	55	51
	C40/50	18	36	45	42

* Prescribed $c_{min,dur}$ for indicative minimum concrete strength class according to [57].

As expected, increasing the concrete class led to a decrease in the cover depth for all exposure classes. The biggest difference was for exposure classes XC1, XC2, and XC3, where it was necessary to increase the minimum cover depth for the indicative minimum class by two times compared to cement concretes of the same strength. However, the values shown in Table 6 enable a simpler application of high-volume limestone powder concretes in terms of durability (carbonation-induced corrosion).

5. Conclusions

Due to the dilution effect of the limestone, the carbonation resistance of the high-volume limestone powder concrete is lower than that of the pure-clinker concrete. This effect can present a limiting factor for the application of the HVLPC in the reinforced concrete structures despite the environmental benefit from significantly reducing the clinker content. Furthermore, the current standards [33,36,57] are not adapted to concrete mixes with such a type of binder.

The property that reflects the concrete carbonation resistance (whether this be the inverse carbonation resistance or carbonation rate coefficient) is determined on the basis of

the measured carbonation depths under defined environmental conditions. Therefore, it has to be experimentally determined, which either is a long-lasting procedure or requires specialized equipment not available in every concrete laboratory. Hence, the attempt was made to establish an empirical relationship between the natural inverse carbonation resistances and mean compressive strength of the HVLPC that is to use the concrete property that has to be tested anyway. To do that, a regression analysis was performed on the experimental results collected from the previous research in the 1995–2023 periods. Applying certain filters on collected data led to 75 experimental results of the carbonation depth measured under natural indoor and sheltered outdoor conditions. Selected data originated from 14 different laboratories. For this analysis, concrete mixes were divided into two groups according to limestone percentage: (1) between 21% and 35%, and (2) between 36% and 70% limestone powder in the concrete powder phase. Based on the linear regression model of the log-transformed variables, empirical relationships were proposed, together with the statistical description of the models. Since the obtained equations for both concrete groups were similar, finally one single correlation was proposed for the whole 21–70% limestone powder content range. The coefficient of determination in this case was equal to 0.78. Keeping in mind the broad range of various parameters in the collected test data, the correlation described with such R^2 can be considered strong enough for the simplified prediction model. It is important to note that the proposed relationships are valid for concrete mixes wet cured for at least 7 days and indoor and outdoor sheltered natural conditions.

A full probabilistic service life analysis regarding the carbonation-induced depassivation of reinforcement was performed using the *fib* Model Code 2010 prediction model and proposed empirical relationship. The analysis was performed for all carbonation exposure classes, commonly applied concrete strength classes (C20/25—C40/50), and service lives of 50 and 100 years. Minimum concrete cover depths for HVLPC were recommended. The obtained results showed that for all exposure classes and both service life durations, the required minimum concrete cover depths $c_{min,dur}$ for HVLPC were significantly larger compared to those prescribed in EN 1992-1-1:2004 for indicative strength classes. For a service life of 50 years, the calculated minimum cover depths were 32 mm for XC1, 46 mm for XC2 and XC3, and 42 mm for XC4. For a service life of 100 years, the calculated cover depths were 48 mm for XC1, 68 mm for XC2, 67 mm for XC3, and 63 mm for XC4. Altogether, the increase varied between 40 and 110%, or between 12 and 33 mm, depending on the exposure class and service life duration. These results clearly indicate that HVLPC should be used for the structures where a service life of 50 years is acceptable. Adding a safety factor of 10 mm for cast-in-situ structures according to EN 1992-1-1:2004 leads to nominal covers of 75–80 mm for a service life of 100 years, which may not be acceptable in practice.

The basic limitations of this study are inherent to every empirical study: its reliability depends on the number and representativeness of the input data. Although analyzed test data originate from a number of different laboratories and cover a wide range of involved parameters, the total number was 75. Increasing the number of experimental results would certainly improve the quality of prognosis. Moreover, as already mentioned, reported results are valid for concrete mixes wet cured for at least 7 days and indoor and outdoor sheltered natural conditions. This is a consequence of the lack of test results. Therefore, more experimental testing of HVLPC carbonation resistance for different curing periods and under different natural conditions is recommended in future research.

The analysis in this study is performed under the assumption that the end-of-service life is the end of the initiation period, when the conditions for the start of corrosion are reached. However, a part of the propagation period, i.e., a certain amount of reinforcement corrosion, can be included in the service life definition, in addition to the initiation (depassivation) period. For instance, that part can be taken as the time until first cracks due to reinforcement corrosion appear. Such a design approach could enable broader HVLPC application in RC structures and should be a subject of the future research.

References

1. IPCC. *AR5 Climate Change 2014: Impacts, Adaptation, and Vulnerability*; IPCC: Geneva, Switzerland, 2014.
2. IPCC. *Global Warming of 1.5 °C*; IPCC: Geneva, Switzerland, 2018.
3. United Nations. *Agreement: United Nations Framework Convention on Climate Change*; United Nations: Paris, France, 2015.
4. Oikonomou, N.D. Recycled concrete aggregates. *Cem. Concr. Compos.* **2005**, *27*, 315–318. [CrossRef]
5. European Parliament. *Amending Energy Performance of Buildings*; Directive (2018/844/EU); European Parliament: Strasbourg, France, 2018.
6. Eurostat. *Generation of Waste by Waste Category, Hazardousness and NACE Rev. 2 Activity*; Eurostat: Luxembourg, 2017.
7. *ISO/TC 07*; Strategic Business Plan. ISO Technical Committee for Concrete, Reinforced Concrete and Prestressed Concrete. ISO: Geneva, Switzerland, 2016.
8. Miller, S.A.; Horvath, A.; Monteiro, P.J.M. Readily implementable techniques can cut annual CO_2 emissions from the production of concrete by over 20%. *Environ. Res. Lett.* **2016**, *11*, 074029. [CrossRef]
9. UN Environment. *Eco-Efficient Cements: Potential Economically Viable Solutions for a Low-CO2 Cement Based Materials Industry*; United Nations Environment Programme: Paris, France, 2017.
10. Gołaszewski, J.; Gołaszewska, M.; Cygan, G. Performance of ordinary and self-compacting concrete with limestone after freeze–thaw cycles. *Buildings* **2022**, *12*, 2003. [CrossRef]
11. Shah, V.; Bishnoi, S. Carbonation resistance of cements containing supplementary cementitious materials and its relation to various parameters of concrete. *Constr. Build. Mater.* **2018**, *178*, 219–232. [CrossRef]
12. Zhang, Z.; Wang, Q.; Chen, H. Properties of high-volume limestone powder concrete under standard curing and steam-curing conditions. *Powder Technol.* **2016**, *301*, 16–25. [CrossRef]
13. Lollini, F.; Redaelli, E. Carbonation of blended cement concretes after 12 years of natural exposure. *Constr. Build. Mater.* **2021**, *276*, 122122. [CrossRef]
14. Soldado, E.; Antunes, A.; Costa, H.; Carmo, R.D.; Júlio, E. Durability of mortar matrices of low-cement concrete with specific additions. *Constr. Build. Mater.* **2021**, *309*, 125060. [CrossRef]
15. Zhang, M.; Lv, H.; Zhou, S.; Wu, Y.; Zheng, X.; Yan, Q. Study on the frost resistance of composite limestone powder concrete against coupling effects of sulfate freeze–thaw. *Buildings* **2023**, *13*, 2776. [CrossRef]
16. Lollini, F.; Redaelli, E.; Bertolini, L. Effects of Portland cement replacement with limestone on the properties of hardened concrete. *Cem. Concr. Compos.* **2014**, *46*, 32–40. [CrossRef]
17. Khokhar, M.; Rozière, E.; Grondin, F.; Loukili, A. Effect of mineral additives on some of durability parameters of concrete. In Proceedings of the 2nd International Conference on Advances in Cement Based Materials and Its Application to Civil Infrastructure, Lahore, Pakistan, 12–14 December 2007; Available online: https://hal.science/hal-01008100 (accessed on 11 December 2023).
18. Collepardi, M.; Collepardi, S.; Olagot, J.J.O.; Simonelli, F. The influence of slag and fly ash on the carbonation of concretes. In Proceedings of the Eighth CANMET/ACI International Conference on Fly Ash, Silica Fume, Slag, and Natural Pozzolans in Concrete, Proceedings ACI SP-221-29, Las Vegas, NV, USA, 23–29 May 2004; pp. 483–494.
19. Meddah, M.S.; Lmbachiya, M.C.; Dhir, R.K. Potential use of binary and composite limestone cements in concrete production. *Constr. Build. Mater.* **2014**, *58*, 193–205. [CrossRef]
20. Elgalhud, A.A.; Dhir, R.K.; Ghataora, G.S. Carbonation resistance of concrete: Limestone addition effect. *Mag. Concr. Res.* **2017**, *69*, 84–106. [CrossRef]
21. Panesar, D.K.; Zhang, R. Performance comparison of cement replacing materials in concrete: Limestone fillers and supplementary cementing materials—A review. *Constr. Build. Mater.* **2020**, *251*, 118866. [CrossRef]
22. Qiu, Q. A state-of-the-art review on the carbonation process in cementitious materials: Fundamentals and characterization techniques. *Constr. Build. Mater.* **2020**, *247*, 118503. [CrossRef]
23. Marinković, M.; Radović, A.; Carević, V. Carbonation of limestone powder concrete: State-of-the-art overview. *Gradjevinski Mater. Konstr. (Build. Mater. Struct.)* **2023**, *66*, 2300005M. [CrossRef]

24. Proske, T.; Hainer, S.; Rezvani, M.; Graubner, C.-A. Eco-friendly concretes with reduced water and cement contents—Mix design principles and laboratory tests. *Cem. Concr. Res.* **2013**, *51*, 38–46. [CrossRef]
25. Palm, S.; Proske, T.; Rezvani, M.; Hainer, S.; Müller, C.; Graubner, C.-A. Cements with a high limestone content—Mechanical properties, durability and ecological characteristics of the concrete. *Constr. Build. Mater.* **2016**, *119*, 308–318. [CrossRef]
26. Neufert, W.; Reuken, I.; Weber, G.; Müller, C.; Palm, S.; Severins, K.; Graubner, C.-A.; Proske, T.; Hainer, S.; Rezvani, M. *Reduzierung der Umweltwirkung der Betonbauweise Durch Neuartige Zemente und Daraus Hergestellter Betone Unter Verwendung Hinreichend Verfügbarer Ausgangsstoffe, Abschlussbericht "Reduzierung der Umweltwirkung der Betonbauweise"*; Deutschen Bundesstiftung Umwelt: Osnabrück, Germany, 2014. (In German)
27. Chen, J.J.; Kwan, A.K.H.; Jiang, Y. Adding limestone fines as cement paste replacement to reduce water permeability and sorptivity of concrete. *Constr. Build. Mater.* **2014**, *56*, 87–93. [CrossRef]
28. Tešić, K.; Marinković, S.; Aleksandar Savić, A. Influence of cement replacement with limestone filler on the properties of concrete. *Gradjevinski Mater. Konstr. (Build. Mater. Struct.)* **2021**, *64*, 165–170. [CrossRef]
29. Fennis, S.A.A.M.; Walraven, J.C. Using particle packing technology for sustainable concrete mixture design. *HERON* **2012**, *57*, 73–101.
30. Kim, Y.-J.; van Leeuwen, R.; Cho, B.-Y.; Sriraman, V.; Torres, A. Evaluation of the efficiency of limestone powder in concrete and the effects on the environment. *Sustainability* **2018**, *10*, 550. [CrossRef]
31. Poudyal, L.; Adhikari, K.; Won, M. Mechanical and durability properties of Portland limestone cement (PLC) incorporated with nano calcium carbonate ($CaCO_3$). *Materials* **2021**, *14*, 905. [CrossRef]
32. Jones, M.; Dhir, R.K.; Newlands, M.; Abbas, A. A study of the CEN test method for measurement of the carbonation depth of hardened concrete. *Mater. Struct.* **2000**, *33*, 135–142. [CrossRef]
33. FIB. *FIB Model Code 2010 Final Draft*; FIB Bulletin; FIB: Lausanne, Switzerland, 2012; Volume 2.
34. Wang, X.-Y. Modeling of hydration, compressive strength, and carbonation of Portland-limestone cement (PLC) concrete. *Materials* **2017**, *10*, 115. [CrossRef] [PubMed]
35. Wang, X.-Y.; Wang, Y.-S.; Lin, R.-S.; Cho, H.-K.; Min, T.-B. Energy optimization design of limestone hybrid concrete in consideration of stress levels and carbonation resistance. *Buildings* **2022**, *12*, 342. [CrossRef]
36. FIB. *FIB Model Code for Service Life Design*; FIB Bulletin; FIB: Lausanne, Switzerland, 2006; Volume 34.
37. *EN 12390-10:2018*; Testing Hardened Concrete—Part 10: Determination of the Carbonation Resistance of Concrete at Atmospheric Levels of Carbon Dioxide. CEN: Brussels, Belgium, 2018.
38. *EN 12390-12:2020*; Testing Hardened Concrete—Part 12: Determination of the Carbonation Resistance of Concrete—Accelerated Carbonation Method. CEN: Brussels, Belgium, 2020.
39. Guiglia, M.; Taliano, M. Comparison of carbonation depths measured on in-field exposed existing r.c. structures with predictions made using fib-Model Code 2010. *Cem. Concr. Compos.* **2013**, *38*, 92–108. [CrossRef]
40. Carević, V.; Ignjatović, I.; Dragaš, J. Model for practical carbonation depth prediction for high volume fly ash concrete and recycled aggregate concrete. *Constr. Build. Mater.* **2019**, *213*, 194–208. [CrossRef]
41. Gonçalves, A.F.; Ribeiro, A.B.; Ferreira, M.E. The new LNEC specifications on reinforced concrete durability. In Proceedings of the International RILEM Workshop on Integrated Service Life Modelling of Concrete Structures, Guimarães, Portugal, 5–6 November 2007; pp. 131–139.
42. Shah, V.; Mackechnie, J.; Scott, A. Determination of carbonation resistance of concrete through a combination of cement content and tortuosity. *J. Build. Eng.* **2022**, *60*, 105176. [CrossRef]
43. Rathnarajan, S.; Dhanya, B.S.; Pillai, R.G.; Gettu, R.; Santhanam, M. Carbonation model for concretes with fly ash, slag, and limestone calcined clay–using accelerated and five-year natural exposure data. *Cem. Concr. Compos.* **2022**, *126*, 104329. [CrossRef]
44. Vu, Q.H.; Pham, G.; Chonier, A.; Brouard, E.; Rathnarajan, S.; Pillai, R.; Gettu, R.; Santhanam, M.; Aguayo, F.; Folliard, K.J.; et al. Impact of different climates on the resistance of concrete to natural carbonation. *Constr. Build. Mater.* **2019**, *216*, 450–467. [CrossRef]
45. Marques, P.F.; Chastre, C.; Nunes, Â. Carbonation service life modelling of RC structures for concrete with Portland and blended cements. *Cem. Concr. Compos.* **2013**, *37*, 171–184. [CrossRef]
46. McNally, C.; Sheils, E. Probability-based assessment of the durability characteristics of concretes manufactured using CEM II and GGBS binders. *Constr. Build. Mater.* **2012**, *30*, 22–29. [CrossRef]
47. Neves, R.; da Fonseca, B.S.; Branco, F.; de Brito, J.; Castela, A.; Montemor, M.F. Assessing concrete carbonation resistance through air permeability measurements. *Constr. Build. Mater.* **2015**, *82*, 304–309. [CrossRef]
48. Belgacem, M.E.; Neves, R.; Talah, A. Service life design for carbonation-induced corrosion based on air-permeability requirements. *Constr. Build. Mater.* **2020**, *261*, 120507. [CrossRef]
49. Radović, A.; Tešić, K. *Experimental Measurement on the Natural Carbonation Depth of Limestone Powder Concrete*; Version 1; Mendeley Data: London, UK, 2023. [CrossRef]
50. Bertolini, L.; Lollini, F.; Redaelli, E. Influence of concrete composition on parameters related to the durability of reinforced concrete structures. In Proceedings of the International RILEM Workshop: Integral Service Life Modelling of Concrete Structures, Guimarães, Portugal, 5–6 November 2007; pp. 71–78.

51. Bertolini, L.; Lollini, F.; Redaelli, E. The effect of ground limestone addition on carbonation and chloride resistance of concrete. In Proceedings of the XII DBMC International Conference on Durability of Building Materials and Components, Porto, Portugal, 12–15 April 2011.

52. Müller, C.; Severins, K.; Hauer, B. New Findings Concerning the Performance of Cements Containing Limestone, Granulated Blast Furnace Slag and Fly Ash as Main Constituents. In *Concrete Technology Reports 2007–2009*; Verlag Bau+ Technik GmbH: Düsseldorf, Germany, 2009.

53. Wang, Q.; Yang, J.; Chen, H. Long-term properties of concrete containing limestone powder. *Mater. Struct.* **2017**, *50*, 168. [CrossRef]

54. Balayssac, J.P.; Détriché, C.H.; Grandet, J. Effects of curing upon carbonation of concrete. *Constr. Build. Mater.* **1995**, *9*, 91–95. [CrossRef]

55. Steiner, S.; Proske, T.; Winnefeld, F.; Lothenbach, B. Effect of limestone fillers on CO_2 and water vapour diffusion in carbonated concrete. *Cement* **2022**, *8*, 100027. [CrossRef]

56. Hunkeler, F.; Lammar, L. Requirements for the Carbonation Resistance of Concrete Mixes; Forschungsauftrag AGB 2008/012 auf Antrag der Arbeitsgruppe Brückenforschung (AGB); Eidgenössisches Departement für Umwelt, Verkehr, Energie und Kommunikation UVEK: Switzerland. 2012. Available online: https://www.tfb.ch/Htdocs/Files/v/6078.pdf/Publikationsliste/HunkelerKarbonatisierungswiderstandvonBetonen2012.pdf (accessed on 11 December 2023). (In German).

57. *EN 1992-1-1:2004*; Eurocode 2: Design of Concrete Structures—Part 1–1: General Rules and Rules for Buildings. CEN: Brussels, Belgium, 2004.

58. von Greve-Dierfeld, S.; Gehlen, C. Performance-Based Durability Design, Carbonation Part 2—Classification of Concrete. *Struct. Concr.* **2016**, *17*, 523–532. [CrossRef]

59. Carević, V.; Ignjatović, I. Limit values of accelerated carbonation resistance to meet EC2 durability requirements. *Građevinski Mater. Konstr. (Build. Mater. Struct.)* **2022**, *65*, 2201001C. [CrossRef]

60. Carević, V.; Ignjatović, I. Evaluation of concrete cover depth for green concretes exposed to carbonation. *Struct. Concr.* **2020**, *22*, 1009–1021. [CrossRef]

61. Kottegoda, N.T.; Rosso, R. *Applied Statistics for Civil and Environmental Engineers*, 2nd ed.; Blackwell Publishing: Oxford, UK, 2008.